and that of DOTAP/Chol liposomes from about 85 nm to 175 nm (data not shown). The ζ-potential of these liposomes was about 50 mV to 60 mV.

For optimization of the charge ratio (+/−) of two types of liposome (DC-Chol/DOPE and DOTAP/Chol) containing Sit-G to pDNA, luciferase activity was measured in HepG2 cells transfected with liposomes at various charge ratios (+/−) in medium with or without serum, as shown in Fig. 2. In the presence of serum, the charge ratio (+/−) in the range of about 2/1 to 3/1 showed the highest transfection efficiency, and particularly at the charge ratio (+/−) of 3/1 in liposomes, the transfection efficiency increased in the presence of serum. DC-Chol/DOPE system in the presence of serum seemed to show higher transfection efficiency than DOTAP/Chol one. Tfx20 showed $1.01 \pm 0.04 \times 10^8$ (RLU/mg protein) luciferase activity at the optimal charge ratio (+/−) of 2/1 when incubated in the medium without serum. Sit-G-liposomes (DC-Chol/DOPE/Sit-G [2/2/1], mole, at the charge ratio [+/−] of 3/1 in Fig. 2) showed comparable transfection efficiency ($1.51 \pm 0.83 \times 10^8$ RLU/mg protein) to that by Tfx20 (charge ratio [+/−]=2/1) even in the presence of serum (Table 1). Inhibition of lipofection by serum has often been reported (Faneca et al., 2004). However, Sit-G-liposomes increased the transfection efficiency despite the presence of serum in the medium. In further studies, therefore we used the DC-Chol/DOPE system and a charge ratio (+/−) of 3/1 of liposome to pDNA as Sit-G-liposomes.

Liposome Formulae Containing MEL

A biosurfactant of MEL produced by yeast has mannose and erythritol residues in its molecule; therefore, we expected that this might also be able to form small-sized lipoplexes

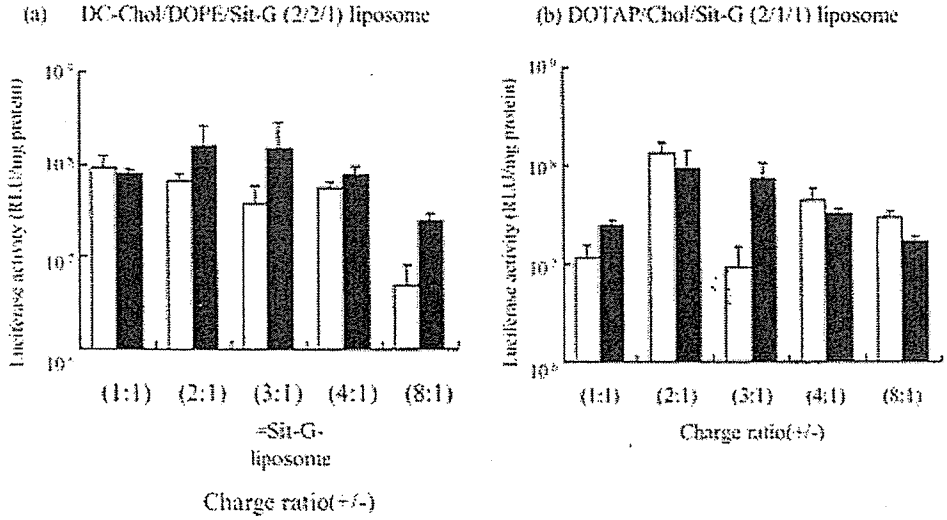

Figure 2. Gene expressions in HepG2 cells transfected with two types of liposomes (DC-Chol/DOPE [a] and DOTAP/Chol [b]) containing Sit-G at various charge ratios (+/−) in medium with or without 10% serum. HepG2 (at a density of 3×10^5 cells/well) was seeded in 12-well plates 24 h before transfection. Liposome/pDNA complexes were diluted with medium with or without serum to a final concentration of 2 μg pDNA in 1 ml medium per well. After transfection in the media without serum for 2 h, 1 ml of the medium was added to the wells and culture was continued for an additional 24 h. For transfection with 10% serum, each cell was incubated for 24 h in medium. Each column represents the mean ± *SD* (n=3–6). (□) without serum; (■) with 10% serum.

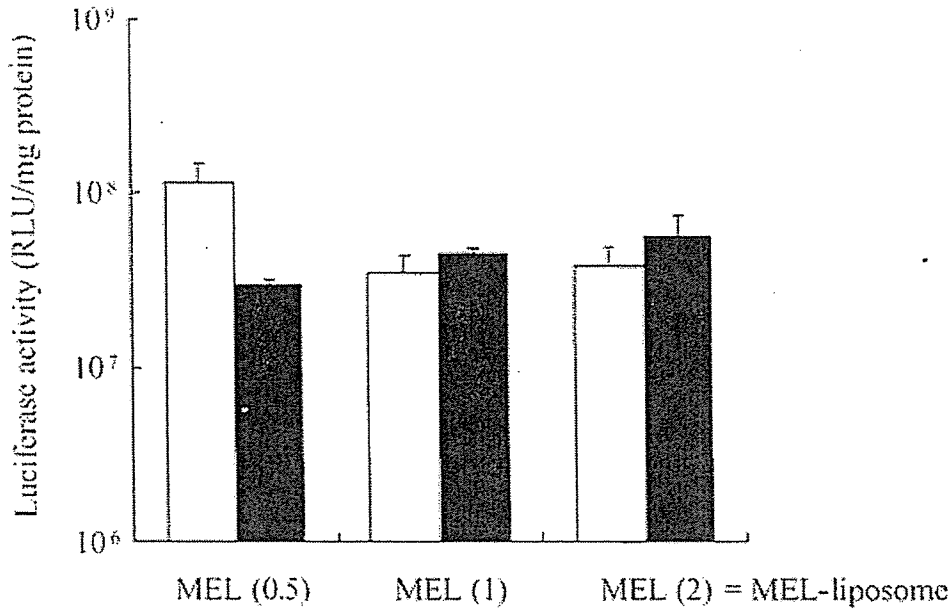

Figure 3. Effect of MEL contained in liposomes (DC-Chol/DOPE/MEL=3/2/0.5–2, molar ratio) on gene expression in HepG2 cells in medium with or without 10% serum. Aliquots of 2 μg of pDNA (pAAV-CMV-luc) were complexed with each liposome at a charge ratio (+/−) of 3 per well. Other experimental conditions were identical to those described in the Fig. 2 legend. Each column represents the mean ± *SD* (n=3–6). MEL (0.5)=DC-Chol/DOPE/MEL=3/2/0.5, molar ratio, MEL (1)=DC-Chol/DOPE/MEL=3/2/1, MEL (2)=DC-Chol/DOPE/MEL=3/2/2. (□) without serum; (■) with 10% serum.

like Sit-G. When the molar ratio of MEL to DC-Chol/DOPE (= 3/2, mole) was changed from 0 to 0.5, 1, and 2 (corresponding to MEL [0], MEL [0.5], MEL [1], and MEL [2] liposomes, respectively), the diameter of liposomes containing MEL was about 80 nm, while liposomes without MEL were about 120 nm in size. These liposome suspensions were stable and could be stored for several months at room temperature without any change in particle size (data not shown).

The effect of MEL in liposomes at various additional ratios of MEL at the charge ratio (+/−) of 3/1 was investigated on gene expression in the medium with or without serum (Fig. 3). When MEL was increased, the transfection efficiency was increased slightly, and MEL (2) showed the highest luciferase activity in the presence of serum. Therefore, in the following studies, we used MEL (2) liposomes as MEL-liposomes.

Control liposomes composed of DC-Chol/DOPE produced aggregation when mixed with pDNA at the charge ratio (+/−) of 3/1, while Sit-G- and MEL-liposomes formed about 300-nm-sized Sit-G- or MEL-lipoplexes, showing high transfection efficiency (Table 1).

Cytotoxicity

We examined the cytotoxicity of liposome vectors (Fig. 4). The concentration of the cationic lipid used in the cell line experiment was about 20 μM in both Sit-G- and MEL-liposomes, resulting in a cell viability of about 70% for Sit-G-lipoplex and 30% for

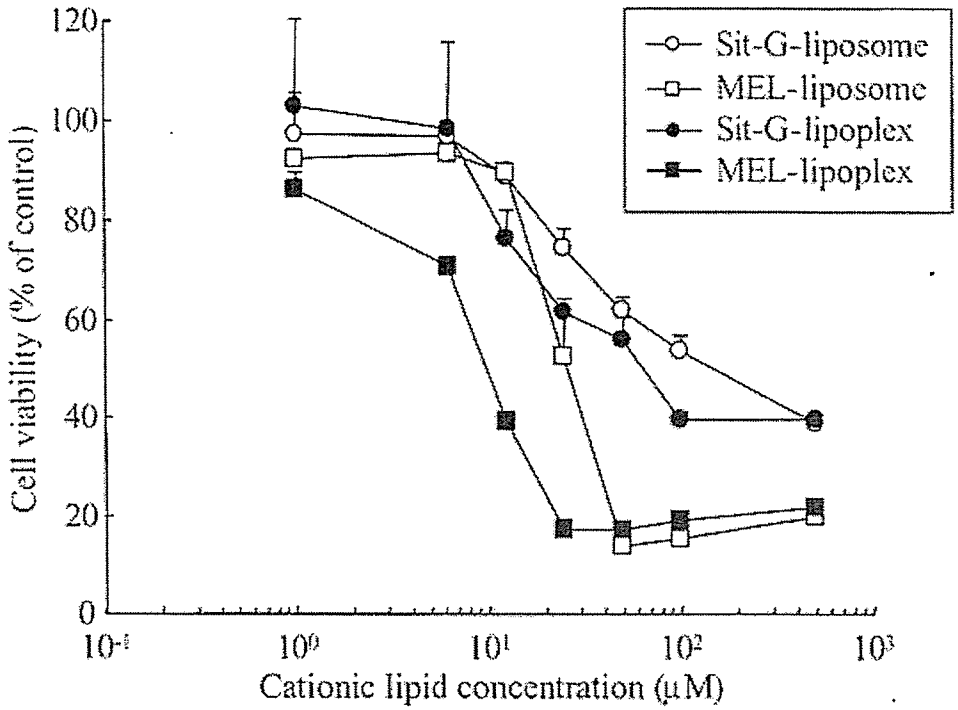

Figure 4. Cytotoxic activity of Sit-G- and MEL-liposomes, and their lipoplexes to HeLa cells. Cells were incubated in medium containing two types of liposomes and lipoplexes for 24 h. Cell viability was determined by WST-8 assay. Data represent the mean ± *SD* (n=4). Sit-G-liposomes: DC-Chol/DOPE/Sit-G=2/2/1 (mole). MEL-liposomes: DC-Chol/DOPE/MEL=3/2/2 (mole). Lipoplex was formed at a charge ratio (+/−) of liposome/DNA=3/1.

MEL-lipoplex. Sit-G- and MEL-liposomes showed decreased cytotoxicity when complexed with pDNA. It might be due to that the positive surface charge of lipoplexes may be decreased by addition of pDNA to liposomes.

In Vitro TK Expression with Liposome Vectors

TK expression by the MK or HSV promoter in HeLa cells was compared by transfection with SitG- and MEL-liposome in medium with 10% serum (Fig. 5). It was confirmed that HeLa cells expressed MK mRNA by RT-PCR analysis (Hattori and Maitani, 2005). Sit-G- and MEL-liposome showed significantly higher pMK-tk activity, about 30 to 40 times than that in nontransduced cells. The Sit-G-liposome showed higher pMK-tk activity than the HSV-tk one.

Suppression of Growth of AsPC-1 Xenografts

It was reported that MK promoter-mediated suicide gene therapy effectively produced cytotoxic effects in AsPC-1 cells (Miyauchi et al., 2001). Therefore, to study the therapeutic potential of liposome vector on the solid tumor model in mice established by AsPC-1 cells, we administered pMK-tk with liposome directly into the tumor and further GCV by i.p. injection (Fig. 6). The treatment schedule consisted of four consecutive intratumoral

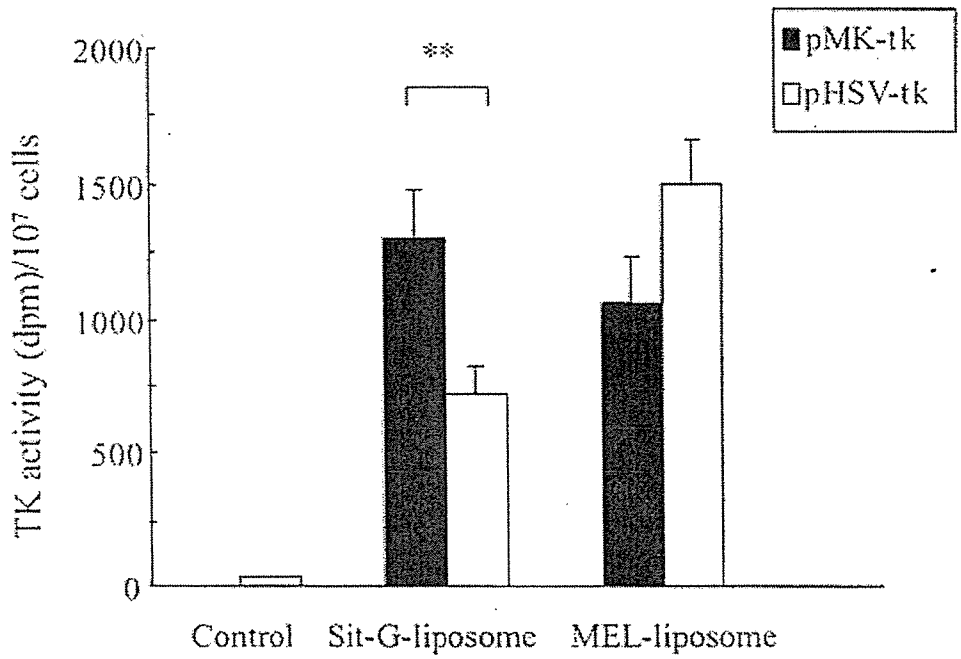

Figure 5. Comparison of TK expression by MK and HSV promoter in HeLa cells transfected with SitG- and MEL-liposome in medium with 10% serum. Cells received no pDNA in control experiments. Aliquots of 2 μg of pDNA (pMK-tk or pHSV-tk) were complexed with each liposome at charge ratio (+/−) of 3 per well. After a 24-h incubation, cells were washed with medium and cell culture was continued for an additional 48 h. Each column represents the mean ± *SD* (n=3). **; $p < .01$.

injections, each of pMK-tk (20 μg/mouse) with two kinds of liposomes or the same volume of PBS as two controls. Of these groups, only the mice treated with transfection by Sit-G-liposome saw delayed tumor growth at 4 to 6 days after starting transfection compared with controls ($p > .05$).

To observe the change in tumor growth for long-term use of Sit-G-liposome, we administered pMK-tk (20 μg/mouse) with Sit-G-liposome or Sit-G-liposome alone directly into the tumor and further GCV by i.p. injection (Fig. 7). The treatment schedule consisted of five consecutive intratumoral injections, each of pMK-tk or the same volume of Sit-G-liposome suspension as a control. The mice treated with transfection of pMK-tk by Sit-G-liposome showed significantly reduced tumor growth compared with those treated with Sit-G-liposome alone at 30 days after starting transfection ($p < .05$). This finding suggested that the antitumor response was caused not by toxicity of Sit-G-liposomes but by transfection of Sit-G-lipoplex against the tumor.

Discussion

Among synthetic vectors, lipoplexes have been the most frequently employed and the most intensively studied. Lipoplexes are large, heterogeneous, and unstable, especially at high pDNA concentrations. They form as a result of electrostatic binding between cationic liposomes and negatively charged pDNA, and they are inherently difficult to manipulate. To protect larger-sized lipoplexes, we prepared initially small-sized liposomes by addition

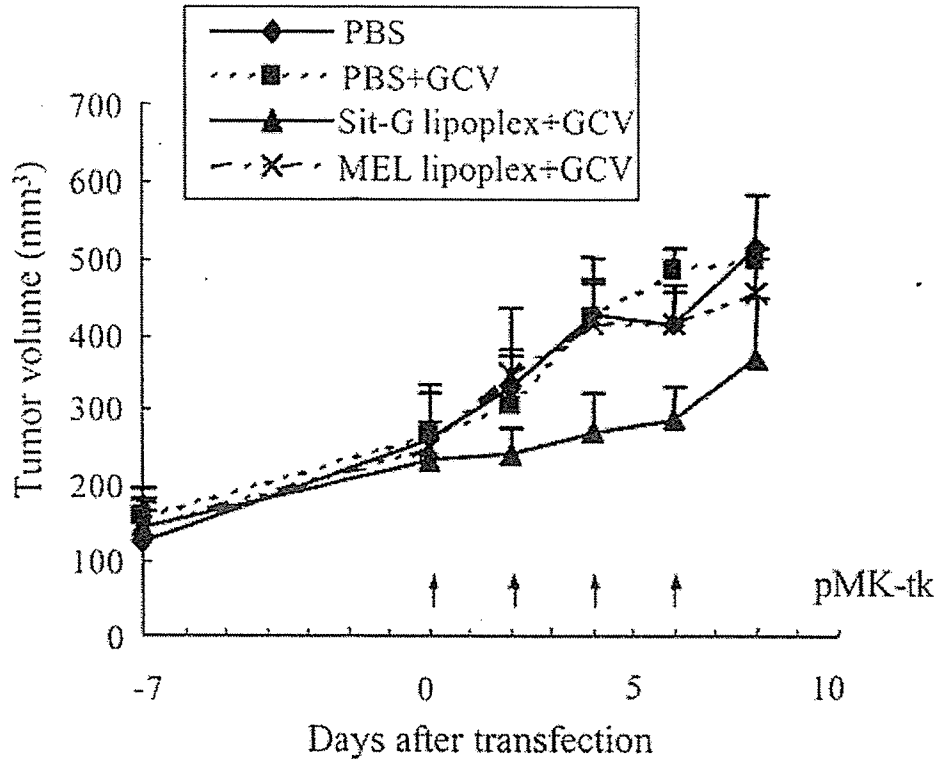

Figure 6. Effect of liposome vectors with pMK-tk administered directly into the tumor on tumor growth in HSV-tk gene therapy. Seven-week-old female BALB/c nude mice were s.c. inoculated with 1×10^6 AsPC-1 cells. On day 0 after inoculation of tumor cells, pMK-tk (20 μg/mouse) with liposome vectors were administered directly into the tumor measuring with 0.6 to 0.7 cm in diameter in animals once every two days 4 times for 7 days. Animals inoculated with liposome vectors were further treated with GCV starting 1 day after gene transfection. GCV was administered by i.p. injection twice a day 4 times for 7 days at a dose of 0.4 mg/mouse/day. Two control groups were treated by injection of PBS (50 μl) instead of pMK-tk and injection either of GCV (0.4 mg/mouse/day) or PBS. Tumor volume was measured using calipers and calculated. Each point represents the mean ± *SE* (n=3–7).

of Sit-G or MEL to DC-Chol/DOPE liposomes and could prepare about 300-nm-sized lipoplexes, whereas lipoplexes of DC-Chol/DOPE liposomes as a control resulted in aggregation in medium with serum. Sit-G and MEL may be good dispersants in preparing lipoplexes.

The early condition of incubation of lipoplexes, with the cells in the presence of serum or not, is important for change of sizes of lipoplexes because large complexes are often more efficient in transfecting cells in vitro (Felgner et al., 1994). The transfection efficiency may be reflected from uptake of lipoplexes to the cells until about 3 h after incubation because transfection was observed 6 h after incubation (data not shown). The transfection efficiency of the luciferase marker gene by Sit-G- and MEL-liposome was enhanced in the presence of serum, comparable to that by Tfx20, a commercial gene transfection reagent in the absence of serum. One of the reasons is that Sit-G may form easily dispersed lipoplexes in the presence of serum (Hwang et al., 2001), suggesting that the glycoside residue in Sit-G molecule prevents the interaction of lipoplexes with serum.

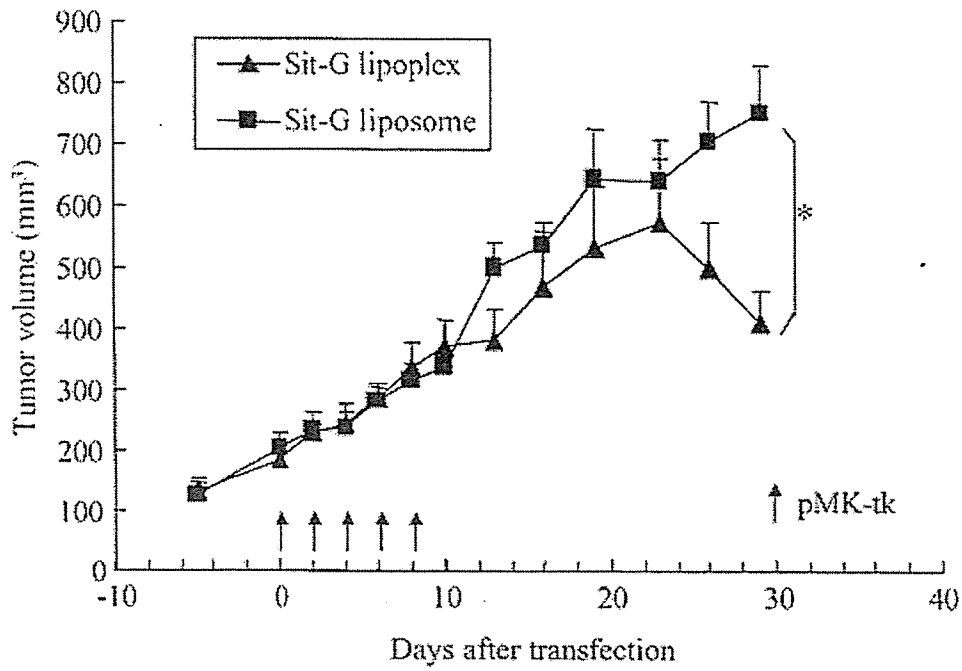

Figure 7. Effect of Sit-G-liposome vector with pMK-tk administered directly into the tumor on tumor growth in HSV-tk gene therapy. Seven-week-old female BALB/c nude mice were s.c. inoculated with 1×10^6 AsPC-1 cells. On day 0 after inoculation of tumor cells, pMK-tk (20 μg/mouse) with liposome vector or liposome alone was administered directly into the tumor measuring with 0.5 to 0.6 cm in diameter in animals once every two days 5 times for 9 days. Animals inoculated with liposome vector were further treated with GCV starting 1 day after gene transfection. GCV was administered by i.p. injection twice a day 5 times for 9 days at a dose of 0.4 mg/mouse/day. Each point represents the mean ± *SE* (n=3–7). *; $p < .05$.

This indicates the usefulness of Sit-G- and MEL-liposomes as transfection reagents. However, the exact mechanism involved in the enhancement of gene expression by serum is not known.

The size of lipoplexes, about 300 nm, seemed rather large, but the lipoplexes can be used for intratumoral and intravenous injection. The size of the lipoplex is an important factor in transfection. Large lipoplexes were reported to contribute to the enhanced gene expression in vitro (Felgner et al., 1994; Zhang et al., 1997; Ross and Hui, 1999; Turek et al., 2000). Here, the size of our lipoplexes was almost 300 nm. Therefore, size effect of transfection may be avoided. Cellular mechanisms of Sit-G- and MEL-liposomes might be different.

In consideration of selectivity and safety, we selected the MK promoter for the application of suicide gene therapy. MK, a growth/differentiation factor, is expressed predominantly in various types of human tumors, whereas its expression in adult normal tissues is highly restricted (Tsutsui et al., 1993). TK expression by pMK-tk mediated by Sit-G- and MEL-liposomes was confirmed in HeLa cells to be comparable to that by pHSV-tk with the HSV promoter. This finding suggested that the MK promoter driving MK-positive cells could achieve tissue-targeted gene expression. Although luciferase expression of Sit-G-liposome was higher than that of MEL-liposome, TK expression by these liposome vectors was not significantly different, not correlating with the luciferase transfection

efficiency. These findings strongly suggested that Sit-G- and MEL-liposomes could be applicable to in vivo HSV-tk gene delivery.

Compared with Sit-G- and MEL-lipoplex, Sit-G-lipoplex was less cytotoxic. Sit-G-liposome reduced significantly tumor size by day 30 after the start of transfection of pMK-tk gene therapy, compared with Sit-G-liposome alone. These findings suggested that cytokines induced by a nonspecific manner by intratumoral injection of lipoplex might not contribute the reduction of the tumor size. The reason that the effect of Sit-G-liposomes on tumor growth suppression was different from that of MEL-liposome vector is not clear, but it might be related to the fact that inhibition of enhanced glucose transport in GCV-treated cells increased apoptosis (Haberkom et al., 2001) with glucose residues in Sit-G in nanoparticles and liposomes (Nakamura et al., 2003). Our finding suggested that HSV-tk gene therapy could be performed by repeated intratumoral administration of Sit-G-liposome vector system. Further study of the optimization of the formulae of Sit-G-liposome and therapeutic design is needed to be used in vivo for this therapy.

We have shown that injectable lipoplexes (about 300 to 350 nm) could be obtained by addition of Sit-G or MEL to cationic liposomes. Smaller-sized Sit-G- and MEL-lipoplexes might be obtained by the dispersity of the sugar residue of Sit-G and MEL in the presence of serum. These liposome vectors showed high transfection of the luciferase gene and TK activity in the cells. Sit-G-liposome is a promising vector in gene-based therapy.

References

Alton, E. W., Geddes, D. M. (1995). Gene therapy for cystic fibrosis: A clinical perspective. *Gene Ther.* 2:88–95.

Egilmez, N. K., Iwanuma, Y., Bankert, R. B. (1996). Evaluation and optimization of different cationic liposome formulations for in vivo gene transfer. *Biochem. Biophys. Res. Commun.* 221:169–173.

Faneca, H., Simoes, S., Pedroso de Lima, M. C. (2004). Association of albumin or protamine to lipoplexes: Enhancement of transfection and resistance to serum. *J. Gene Med.* 6:681–692.

Felgner, J. H., Kumar, R., Sridhar, C. N., Wheeler, C. J., Tsai, Y. J., Border, R., Ramsey, P., Martin, M., Felgner, P. L. (1994). Enhanced gene delivery and mechanism studies with a novel series of cationic lipid formulations. *J. Biol. Chem.* 269:2550–2561.

Gao, X., Huang, L. (1996). Potentiation of cationic liposome-mediated gene delivery by polycations. *Biochemistry* 35:1027–1036.

Haberkom, U., Altmann, A., Kamencic, H., Morr, I., Traut, U., Henze, M., Jiang, S., Metz, J., Kinschent, R. (2001). Glucose transport and apoptosis after gene therapy with HSV thymidine kinase. *Eur. J. Nucl. Med.* 28:1690–1696.

Hamy, F., Verwaerde, P., Helbecque, N., Formstecher, P., Henichart, J. P. (1991). Nuclear targeting of a viral-cointernalized protein by a short signal sequence from human retinoic acid receptors. *Bioconjug. Chem.* 2:375–378.

Hattori, Y., Maitani, Y. (2006). Two-step transcriptional amplification-lipid-based nanoparticles using PSMA or midkine promoter for suicide gene therapy in prostate cancer. *Cancer Sci.* 97:787–798.

Hayashi, K., Hayashi, T., Sun, H. D., Tanaka, Y. (2000). Potentiation of ganciclovir toxicity in the herpes simplex virus thymidine kinase/ganciclovir administration system by ponicidin. *Cancer Gene Ther.* 7:45–52.

Hwang, S. H., Hayashi, K., Maitani, Y. (2001). Liver-targeted gene transfer into a human hepatoblastoma cell line and in vivo by sterylglucoside-containing cationic liposomes. *Gene Ther.* 8:1276–1280.

Inoh, Y., Kitamoto, D., Hirashima, N., Nakanishi, M. (2001). Biosurfactants of MEL-A increase gene transfection mediated by cationic liposomes. *Biochem. Biophys. Res. Commun.* 289:57–61.

Kawakami, S., Sato, A., Nishikawa, M., Yamashita, F., Hashida, M. (2000). Mannose receptor-mediated gene transfer into macrophages using novel mannosylated cationic liposomes. *Gene Ther.* 7:292–299.

Lai, E., van Zanten, J. H. (2002). Real time monitoring of lipoplex molar mass, size and density. *J. Control. Release* 82:149–158.

Li, S., Rizzo, M. A., Bhattacharya, S., Huang, L. (1998). Characterization of cationic lipid-protamine-DNA(LPD) complexes for intravenous gene delivery. *Gene Ther.* 5:930–937.

Maitani, Y., Soeda, H., Wang, J., Takayama, K. (2001). Modified ethanol injection method for liposomes containing β-sitosterol β-D-glucoside. *J. Liposome Res.* 11:115–125.

Miller, N., Whelan, J. (1997). Progress in transcriptionally targeted and regulatable vectors for genetic therapy. *Hum. Gene Ther.* 8:803–815.

Miyauchi, M., Yoshida, Y., Tada, Y., Narita, M., Maeda, T., Bahar, R., Kadomatsu, K., Maramatsu, T., Matsubara, S., Nakagawara, A., Sakiyama, S., Tagawa, M. (2001). Expression of herpes simplex virus-thymidine kinase gene controlled by a promoter region of the midkine gene confers selective cytotoxicity to ganciclovir in human carcinoma cells. *Int. J. Cancer* 91:723–727.

Nakamura, K., Maitani, Y., Takayama, K. (2003). Regional intestinal absorption of FITC-dextran 4,400 with nanoparticles based on β-sitosterol β-D-glucoside in rats. *J. Pharm. Sci.* 92:311–318.

Park, J. Y., Elshami, A. A., Amin, K., Rizk, N., Kaiser, L. R., Albelda, S. M. (1997). Retinoids augment the bystander effect in vitro and in vivo in herpes simplex virus thymidine kinase/ganciclovir-mediated gene therapy. *Gene Ther.* 4:909–917.

Perrie, Y., Gregoriadis, G. (2000). Liposome-entrapped plasmid DNA: Characterization studies. *Biochim. Biophys. Acta.* 1475:125–132.

Ross, P. C., Hui, S. W. (1999). Lipoplex size is a major determinant of in vitro lipofection efficiency. *Gene Ther.* 6:651–659.

Shimizu, K., Maitani, Y., Takayama, K., Nagai, T. (1996). Characterization of dipalmitoylphosphatidylcholine liposomes containing a soybean-derived sterylglucoside mixture by differential scanning calorimetry, Fourier transform infrared spectroscopy and enzymatic assay. *J. Pharm. Sci.* 85:741–744.

Sternberg, B., Sorgi, F. L., Huang, L. (1994). New structures in complex formation between DNA and cationic liposomes visualized by freeze-fracture electron microscopy. *FEBS Lett.* 356:361–366.

Tsutsui, J., Kadomatsu, K., Matsubara, S., Nakagawara, A., Hamanoue, M., Takao, S., Shimazu, H., Ohi, Y., Muramatsu, T. (1993). A new family of heparin-binding growth/differentiation factors: increased midkine expression in Wilms' tumor and other human carcinomas. *Cancer Res.* 53:1281–1285.

Turek, J., Dubertret, C., Jaslin, G., Antonakis, K., Scherman, D., Pitard, B. (2000). Formulations which increase the size of lipoplexes prevent serum-associated inhibition of transfection. *J. Gene Med.* 2:32–40.

Wang, J., Guo, X., Xu, Y., Barron, L., Szoka, F. C., Jr. (1998). Synthesis and characterization of long chain alkyl acyl carnitine esters. Potentially biodegradable cationic lipids for use in gene delivery. *J. Med. Chem.* 41:2207–2215.

Wheeler, V. C., Coutelle, C. (1995). Nondegradative in vitro labeling of plasmid DNA. *Anal. Biochem.* 225:374–376.

Zadi, B., Gregoriadis, G. (2000). A novel method for high-yield entrapment of solutes into small liposomes. *J. Liposome Res.* 10:73–80.

Zhang, Y. P., Reimer, D. L., Zhang, G., Lee, P. H., Bally, M. B. (1997). Self-assembling DNA-lipid particles for gene transfer. *Pharm. Res.* 14:190–196.

Comparison of the Glass Transition Temperature and Fragility Parameter of Isomalto-Olygomer Predicted by Molecular Dynamics Simulations with Those Measured by Differential Scanning Calorimetry

Sumie YOSHIOKA* and Yukio ASO

National Institute of Health Sciences; 1–18–1 Kamiyoga, Setagaya-ku, Tokyo 158–8501, Japan.
Received July 19, 2005; accepted August 21, 2005; published online August 23, 2005

The purpose of this study is to examine whether molecular dynamics (MD) simulations using a commercially available software for personal computers can estimate the glass transition temperature (T_g) of amorphous systems containing pharmaceutically-relevant excipients. MD simulations were carried out with an amorphous matrix model constructed from isomaltoheptaose, and the T_g estimated from the calculated density *versus* temperature profile was compared with the T_g measured by differential scanning calorimetry (DSC) for freeze-dried isomalto-oligomer having an average molecular weight close to that of isomaltoheptaose. The T_g values determined by DSC were lower by 10 to 20 K than those extrapolated from the T_g values estimated by MD simulation. Fragility parameter was estimated to be 56 and 51 from MD simulation and from DSC measurement, respectively. Thus, the results suggest that MD simulation can provide approximate estimates for the T_g and fragility parameter of amorphous formulations. However, a reduction of the cooling rate, achievable by sufficiently elongating the simulation duration, is necessary for more accurate estimation.

Key words molecular dynamics simulation; amorphous; glass transition; fragility; lyophilization

Glass transition temperature (T_g) is an important property for amorphous pharmaceutical formulations, because it is closely related to the storage stability. The T_g of amorphous materials can usually be determined by calorimetry, but this technique cannot be applied to amorphous formulations containing polymers with widely distributed molecular weights. This is because these formulations often exhibit unclear changes in heat capacity at T_g due to the glass transition occurring over a wide temperature range. Molecular dynamics (MD) simulations can be performed for an amorphous matrix model constructed using polymer molecules of a uniform molecular weight, in which the chemical structure of the repeated unit can be modified. If T_g prediction is possible based on MD simulations, the dependence of T_g on the polymer molecular weight as well as on the chemical structure of the repeated unit can therefore be elucidated, leading to the efficient development of polymer excipients with high T_g values suitable for stable amorphous dosage forms. Furthermore, MD simulations can determine the dependence of fragility for polymer matrices on the polymer molecular weight and on the chemical structure of the repeated unit. Thus, it would be possible to estimate the fragility parameter of polymer matrices with widely distributed molecular weights, which usually cannot be determined from the heating-rate dependence of T_g nor from the width of glass transition.

MD simulations have been utilized to estimate the glass transition temperature (T_g) of amorphous synthetic polymers,[1,2] glass former saccharides and concentrated saccharide–water systems.[3—8] These studies suggest that MD simulations are useful in estimating the T_g of amorphous materials. Our previous MD simulations with isomaltodecaose (a fragment of dextran) and α-glucose (the repeated unit of dextran) demonstrated that MD simulations can provide rational T_g values that decrease upon hydration and increase with increasing fragment size, suggesting the usefulness of MD simulations.[9] However, the T_g obtained from MD simulations was not compared with experimentally determined T_g, in consideration of the heating/cooling-rate dependence. Such comparison is necessary in order to evaluate the reliability of MD simulations.

In this study, the T_g of an isomalto-oligomer of relatively narrow molecular weight distribution was determined as a function of heating and cooling rates by differential scanning calorimetry (DSC). For the other angle of investigation, MD simulations were carried out with an amorphous matrix constructed from isomaltoheptaose, the molecular weight of which was close to the isomalto-oligomer investigated. The density of the isomaltoheptaose matrix was calculated as a function of temperature, and the T_g of the matrix was estimated from a change in the slope of the density *versus* temperature profile. The T_g estimates obtained at various cooling rates were compared with the experimental data in order to examine whether MD simulations using a commercially available software for personal computers can provide reliable T_g estimates for amorphous systems containing pharmaceutically-relevant excipients.

Experimental

DSC Measurement Isomalto-oligomer (number average molecular weight (Mn) of 1010; a polydispersity index (Mw/Mn) of 1.26) was purchased from Fluka Production GmbH (Switzerland). Four hundred microliters of 2.5% w/w isomalto-oligomer solution was frozen in a polypropylene sample tube (10 mm diameter) by immersion in liquid nitrogen for 10 min. Freeze drying was carried out at a vacuum level below 5 Pa for 23.5 h in a lyophilizer (Freezevac C-1, Tozai Tsusho Co., Tokyo). The shelf temperature was between −35 and −30 °C for the first 1 h, 20 °C for the subsequent 19 h, and 30 °C for the last 3.5 h. Residual water was less than the detection limit of the Karl Fisher method.

The T_g of lyophilized samples was measured by DSC (2920, TA Instruments, New Castle, DE, U.S.A.). Samples were heated in aluminum pans to 40 °C higher than the T_g, and then cooled to 40 °C lower than the T_g at a cooling rate of 2, 5 and 10 °C/min with a refrigeration system or at a cooling rate of 20 and 40 °C/min with a liquid nitrogen cooling accessory. Then, samples were heated again at a heating rate of 2, 5, 10, 20 and 40 °C/min. Temperature calibration was carried out using indium at each heating rate. The T_g was recorded as the middle of the change in heat capacity at the glass

* To whom correspondence should be addressed. e-mail: yoshioka@nihs.go.jp

transition.

Molecular Dynamics Simulation A model system for the amorphous isomalto-oligomer was built using the software package Amorphous Cell Construction (Material Studio, MSI Inc.). A periodic cell containing 7 isomaltoheptaose molecules was constructed by the minimization procedure using the Steepest Descents and Conjugate Gradients (5000 steps). For comparison with the isomaltoheptaose system, a periodic cell containing 49 α-glucose molecules was also constructed.

Isothermal-isobaric molecular dynamics simulations (NPTMD) were carried out with the constructed systems using the software package DISCOVER with the Polymer Consortium Force Field. The Velocity Verlet algorithm was used for integration. Interaction between non-bonded atoms was represented in van der Waals and Coulombic terms. Summation methods for van der Waals and Coulomb interactions were atom based and group based, respectively (cutoff of 12.50 A, spline width of 3.00 A, and buffer width of 1.00 A). Charge groups were defined in two different types. In type 1, the entire glucose unit was defined as a group. In type 2, five groups were defined (three groups were comprised of hydroxymethine at positions 2, 3 and 4, respectively, one group was comprised of C1, H1 and the ring O, and one group was comprised of the C5 methine, C6 methylene and O6), as shown in Chart 1. The different group definitions did not cause significant differences in the T_g values estimated, as described later.

A series of simulations was performed with temperatures decreased by intervals of 10 K from 673 to 353 K at a pressure of 0.1 MPa. Temperature and pressure were controlled by the Anderson procedure. The length of simulation at each temperature was 25, 100, 250 ps, or 1 ns with a step size of 1 fs, such that cooling rate was 0.4, 0.1, 0.04 or 0.01 K/ps, respectively. Each subsequent simulation was started from the final configuration obtained at the preceding temperature. System configurations were stored every 5000 steps. The density at each temperature was calculated from the average specific volume observed for the final third of the simulation span at the temperature. The series of simulations from 673 to 353 K was repeated 3 times

The calculated density was plotted against temperature, and the low-temperature and high-temperature portions of the data were fitted with straight lines. T_g was estimated from the point that deviated from the straight line in the low-temperature range and overlapped the straight line in the high-temperature range.

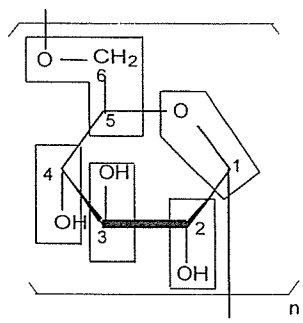

Chart 1. Five Charge Groups in the Repeated Unit of Isomaltoheptaose Defined for the Calculation of Coulomb Interaction

Results and Discussion

Figure 1 shows the density of the amorphous isomaltoheptaose system calculated by NPTMD at cooling rates of 0.4, 0.1, 0.04 and 0.01 K/ps as a function of temperature. The density *versus* temperature plots exhibit a change in the slope at a temperature corresponding to the T_g. As cooling rate decreased, variation in the density data decreased, showing more obvious changes in the slope.

T_g was estimated from the density *versus* temperature plots, and the results are plotted against cooling rate in Fig. 2. Figure 2 also shows T_g values measured by DSC for an isomalto-oligomer having a Mn of 1010 (close to the Mn of isomaltoheptaose, 1152). The T_g values measured during cooling were slightly lower than those measured during heating (the former overlapped with the latter at the two points of higher cooling/heating rate). The solid line in Fig. 2 represents a regression curve for the cooling-rate dependence of the T_g estimated by MD simulation (Type 1). The dotted line represents that of the T_g determined by DSC. Fragility parameters (m) were calculated according to Eq. 1[12] using the

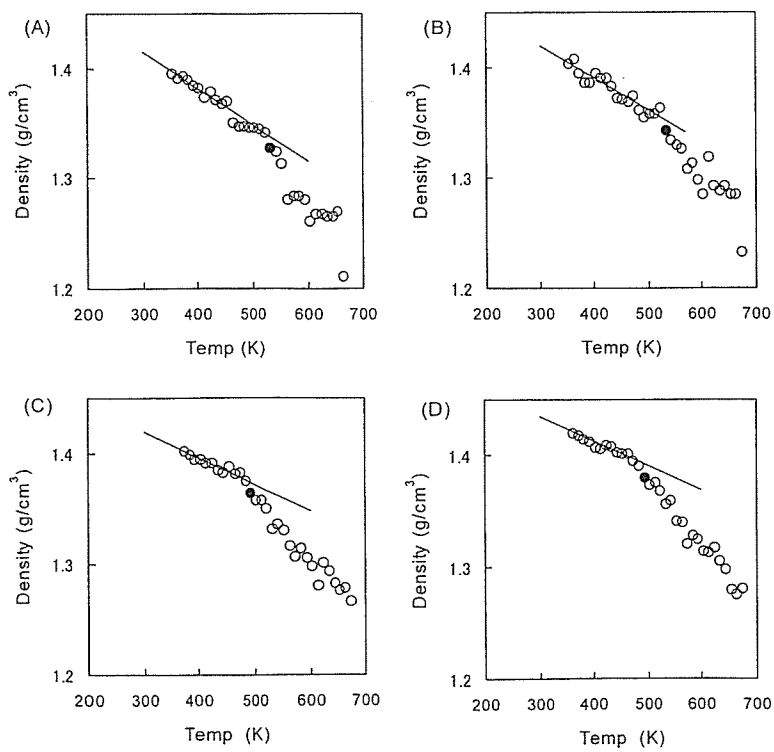

Fig. 1. Density *versus* Temperature Plots Obtained by NPTMD at Cooling Rates of 0.4 K/ps (A), 0.1 K/ps (B), 0.04 K/ps (C) and 0.01 K/ps (D)
Solid circles indicate estimated T_g.

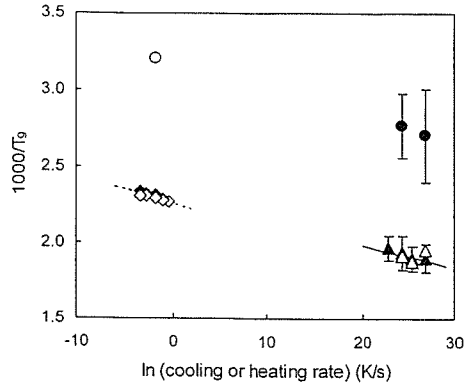

Fig. 2. Cooling-Rate Dependence of T_g Estimated from Density *versus* Temperature Plots for Amorphous α-Glucose (●) and Isomaltoheptaose (Type 1 Group ▲, Type 2 Group △) is Compared with the Heating-Rate Dependence of T_g Measured by DSC for Amorphous α-Glucose (○) and Isomalto-Oligomer (◇), and with the Cooling-Rate Dependence of T_g Measured by DSC for Amorphous Isomalto-Oligomer (◆)

The solid line and dotted line represent regression curves for the cooling-rate dependence of estimated T_g values and that of measured T_g values, respectively. Error bars for ● and ▲ represent S.D. (n=3).

slope of the regression curves and the T_g values at a cooling rate of 20 K/s (DSC measurement) and 4×10^{10} K/s (MD simulation).

$$m \cong \frac{1}{2.303T_g}\frac{d(\ln q)}{d(1/T_g)} \quad (1)$$

where q is the experimental heating or cooling rate. m was estimated to be 56 and 51 from MD simulation and from DSC determination, respectively. These values appeared to be reasonable in comparison with the values reported for various amorphous organic compounds.[12]

The dependence of T_g on the cooling rate (q) can be described by Eq. 2, if the relaxation time of the system shows a Vogel–Fulcher dependence on temperature.[13,14]

$$T_g = T_0 - \frac{B}{\ln(Aq)} \quad (2)$$

where A and B are constants and T_0 is the glass transition temperature when q approaches zero. Curve-fitting of the T_g estimated in the present MD simulation to Eq. 2 provided a regression curve shown in Fig. 3 (T_0, A and B were estimated to 421 K, 10^{-16} and 1150, respectively). The experimentally determined T_g values were lower than the extrapolated values by 10 to 20 K. This small difference suggests that MD simulation can provide approximate estimates of T_g and m, along with the fact that similar m values (56, 51) were estimated from MD simulation and from DSC measurement, respectively.

The lack of complete accordance between the T_g and m values estimated from MD simulation and those obtained from DSC measurement may be attributed to the short simulation duration (*i.e.*, the large cooling rate of 0.01—0.4 K/ps) used in the present study, in which density was not calculated at cooling rates slower than 0.01 K/ps because approximately 100 h of computing time were needed for an NPTMD of 1 ns duration. Decreasing the cooling rate (*i.e.*, prolonging the simulation duration) by using a more powerful computer would provide more reliable estimates of T_g and m. Furthermore, the difference between the estimated T_g and the experimentally determined T_g may result from the difference in parameter used in these two methods (*i.e.*, density in MD simulation *versus* heat capacity in DSC). Therefore, this effect needs to be elucidated for more precise estimation of T_g and m.

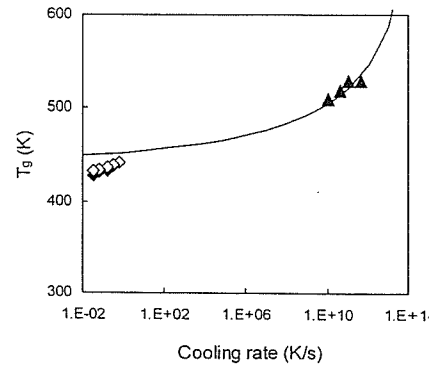

Fig. 3. Curve-Fitting of T_g Estimated from Density *versus* Temperature Plots for Isomaltoheptaose (Type 1 Group) ▲ According to Eq. 2

T_g for isomalto-oligomer determined by DSC during heating (◇) and during cooling (◆) are shown.

Figure 2 also compares the T_g of α-glucose measured by DSC with that estimated by MD simulation. The T_g estimates for α-glucose were lower than those for isomaltoheptaose, correctly reflecting a decrease in molecular weight. Although regression analysis could not be performed with this limited number of data, the relationship between the T_g from DSC measurement and from MD simulations appeared similar to that observed for the isomalto-oligomer.

Conclusions

The T_g of isomaltoheptaose estimated by MD simulation was compared with the T_g determined by DSC for isomalto-oligomer having a close Mn, in order to examine whether MD simulations using a commercially available software for personal computers can provide reliable T_g estimates of amorphous systems containing pharmaceutically-relevant excipients. The results suggest that MD simulation can provide approximate estimates for the T_g and m of amorphous formulations. However, a reduction of the cooling rate, achievable by sufficiently elongating the simulation duration, is necessary for more accurate estimation.

References

1) Han J., Gee R. H., Boyd R. H., *Macromolecules*, **27**, 7781—7784 (1994).
2) Tsige M., Taylor P. L., *Phys. Rev. E*, **65**, 021805-1-8 (2002).
3) Momany F. A., Willett J. L., *Biopolymers*, **63**, 99—110 (2002).
4) Conrad P. B., de Pablo J. J., *J. Phys. Chem. A*, **103**, 4049—4055 (1999).
5) Ekdawi-Sever N. C., Conrad P. B., de Pablo J. J., *J. Phys. Chem. A*, **105**, 734—742 (2001).
6) Caffarena E. R., Grigera J. R., *Carbohydr. Res.*, **315**, 63—69 (1999).
7) Caffarena E. R., Grigera J. R., *Carbohydr. Res.*, **300**, 51—57 (1997).
8) Roberts C. J., Debenedetti P. G., *J. Phys. Chem. B*, **103**, 7308—7318 (1999).
9) Yoshioka S., Aso Y., Kojima S., *Pharm. Res.*, **20**, 873—878 (2003).
10) Debenedett P. G., "Metastable Liquids, Consepts and Principles," Princeton University Press, Princeton, 1996.
11) Angell C. A., Torell L. M., *J. Chem. Phys.*, **78**, 937—945 (1983).
12) Crowley K. J., Zografi G., *Thermochimica Acta*, **380**, 79—93 (2001).
13) Vollmayr K., Kob W., Binder K., *J. Chem. Phys.*, **105**, 4714—4728 (1996).
14) Caprion D., Schober H. R., *J. Chem. Phys.*, **117**, 2814—2818 (2002).

Effect of Freezing Rate on Physical Stability of Lyophilized Cationic Liposomes

Yukio Aso* and Sumie Yoshioka

National Institute of Health Sciences; 1–8–1 Kamiyoga, Setagaya, Tokyo 158–8501, Japan.
Received October 1, 2004; accepted December 8, 2004; published online December 16, 2004

Factors affecting the storage stability of lyophilized cationic liposomes were investigated using liposomes prepared with various excipients and by different freezing rates, either quick freezing (freezing by immersion into liquid nitrogen) or slow freezing (cooling to −50 °C at a rate of −10 °C/h). Increases in the particle size of cationic liposomes observed during freeze-drying were inhibited by the addition of sucrose, trehalose and sucrose–dextran mixtures (1 : 1 and 2 : 1 by weight). The storage instability of the formulations, as indicated by changes in particle size, was affected by their glass transition temperature (T_g). Addition of high-T_g excipients resulted in smaller increases in the particle size, indicating improvement of storage stability. The storage stability of cationic liposome formulations was also affected by freezing rate. Formulations prepared by slow freezing exhibited better stability. Longer shear relaxation times were observed for formulations prepared by slow freezing compared with those prepared by quick freezing. This indicates that formulations prepared by slow freezing have a lower matrix mobility, which may result in better storage stability. T_g or ^{1}H-NMR relaxation measurements could not detect differences in matrix mobility between formulations prepared by different freezing rates. Shear relaxation measurements seem to be a useful method for evaluating the storage stability of cationic liposome formulations.

Key words cationic liposome; stability; lyophilization; shear relaxation time; molecular mobility

Cationic lipid has attracted much attention as a non-viral DNA vector. Cationic liposome–DNA complex (lipoplex), however, is usually unstable in solution and forms aggregates during long-term storage at room temperature, resulting in the loss of its transfection ability.[1,2] Stability of lipoplex during freeze-drying and subsequent storage can be improved by lyophilization with lyoprotectants such as sucrose.[3—5] The stabilizing effect of these compounds on liposomes during lyophilization has been attributed to incorporation of liposomes into glass matrices and hydrogen bonding between the excipient and the polar head group of lipids.[6] Therefore, the storage stability of lyophilized cationic liposomes is expected to be improved by addition of excipients with higher glass transition temperature (T_g), which yield glass matrices with a lower molecular mobility.

It is also known that process parameters such as freezing rate affect the stability of lyophilized formulations. It has been reported that the amount of drug entrapped in lyophilized liposomes is higher for formulations prepared by slow freezing than for those prepared by quick freezing.[7] The effect of freezing rate depended on the lipid composition and was most pronounced for rigid liposomes. The storage stability of lyophilized tissue-type plasminogen activator was also affected by freezing rate.[8] Faster freezing caused a larger surface area of the freeze-dried cake, and the storage stability of the incorporated protein was proportional to the surface area of the freeze-dried cake.

This paper describes the effects of excipients with different T_g as well as the effect of freezing rate on the storage stability of lyophilized cationic liposomes. Changes in the particle size of cationic liposomes were determined as a measure of storage instability. ^{1}H-NMR relaxation time and shear relaxation time of the freeze-dried cakes were also determined. The storage stability of cationic liposomes is discussed in terms of the molecular mobility and visco-elastic property (matrix mobility) of the freeze-dried cakes.

Experimental

Materials *N*-[1-(2,3-Dioleoyloxy) propyl]-*N*,*N*,*N*-trimethyl-ammonium chloride (DOTAP), cholesterol, sucrose, trehalose and dextran were purchased from Sigma (St. Louis, MO, U.S.A.).

Preparation of Cationic Liposomes[3] DOTAP (250 mg) and cholesterol (125 mg) were dissolved in chloroform (about 5 ml). The chloroform was evaporated with a stream of nitrogen gas to make a thin film of the lipids. The film was further dried under vacuum for 1 h and hydrated in 50 ml of water. The lipid suspension was incubated at 50 °C for 10 min and extruded through polycarbonate membranes (Millipore, Billerica, MA, U.S.A.) with pore sizes of 0.6 and 0.2 μm, which were connected in series.

Preparation of Lyophilized Liposome Formulations Sucrose, trehalose and sucrose–dextran mixtures (1 : 1 or 2 : 1 by weight) were used as excipients for lyophilized liposome formulations. Equal volumes of excipient solution (10 w/w%) and liposome suspension were mixed. Aliquots (500 μl) of the mixture were frozen in polypropylene tubes by immersion into liquid nitrogen (quick freezing) or by cooling on the shelf of a freeze drier (Freezevac C-3; Tozai Tsusho, Tokyo) at a rate of −10 °C/h to −50 °C (slow freezing). Frozen samples were dried under a vacuum of approximately 5 Pa. The shelf temperature was maintained at −40 °C for 24 h, −20 °C for 16 h, 0 °C for 6 h, and then 20 °C for 6 h.

Stability Study of Lyophilized Cationic Liposomes The water content of the lyophilized formulations was adjusted by storage at 25 °C and 23% RH for 1 d. The samples were stored at 40 or 25 °C in a thermostatic chamber and withdrawn at appropriate intervals. The storage stability of liposomes was evaluated from changes in particle size. Particle size was determined at 25 °C by dynamic light scattering with a DLS-7000 system (Otsuka Electronics Co. Ltd., Osaka). The viscosity of the rehydrated liposome suspension, required for the calculation of particle size, was determined with a model AR-1000 rheometer (TA Instruments, Inc., New Castle, DE, U.S.A.). The T_g values of the formulations are summarized in Table 1.

Physicochemical Properties of Lyophilized Liposome Formulations. Determination of the Complex Shear Modulus The visco-elastic property (matrix mobility) of the freeze-dried cakes was examined with the model AR-1000 rheometer. A freeze-dried cake was placed on the sample platform of the instrument and compressed to about 440 μm thickness with a flat plate geometry (40 mm in diameter). An oscillating stress of 40 Pa was applied to the sample over a frequency range of 0.01 to 600 radian/s. The effect of sample size, which was smaller than the plate size of the geometry used, on the determination of shear relaxation time was considered to be negligible, since shear relaxation time was estimated from relative changes in the shear modulus determined as a function of stress frequency.

^{1}H-NMR Relaxation Measurements In order to determine the molecu-

* To whom correspondence should be addressed. e-mail: aso@nihs.go.jp

lar mobility of the freeze-dried cakes, spin–lattice relaxation times in laboratory frame (T_1) and rotating frame ($T_{1\rho}$) were measured at 27 °C with a model JNM-MU25 spectrometer (JEOL DATUM, Tokyo) operated at a ^1H resonance frequency of 25 MHz. A freeze-dried cake was placed in an NMR tube (10 mm outer diameter) and dried at 25 °C for 18 h under vacuum before measurement. T_1 was measured by the inversion-recovery method. A spin locking field of 1 mT was applied to the samples for $T_{1\rho}$ measurement.

DSC Analysis The T_g of freeze-dried cakes was determined with a model 2920 differential scanning calorimeter (TA Instruments, Inc.) equipped with a refrigerator cooling accessory. Temperature and heat flow calibration of the instrument was performed with indium. Approximately 3 mg of freeze-dried cake was weighed into a hermetic sample pan, which was stored at 25 °C and 23% RH for 24 h and then sealed. Samples were heated at a rate of 20 °C/min from −30 to 200 °C. The DSC cell was purged with nitrogen gas at 30 ml/min during measurement.

Water Vapor Sorption Measurements Time profiles of water vapor sorption for lyophilized liposome formulations containing sucrose and trehalose were measured at 25 °C and 10% RH with a GM-300 gravimetric sorption analyzer (VTI Corp., Hialeah, FL, U.S.A.). Approximately 25 mg of freeze-dried cake was placed in a sample holder and dried at 25 °C under vacuum. When no change in the weight of the cake was observed over 5 min, the cake was considered to be in a dry state. The cake was exposed to water vapor equivalent to 10% RH. The weight of the cake was measured at intervals of 30 s.

Results and Discussion

Effect of Excipients on Stability of Lyophilized Cationic Liposomes Figure 1 shows the effect of freeze-thaw and freeze-drying on the particle size of cationic liposomes. No significant difference in particle size was observed after the freeze-thaw cycle, regardless of the presence of excipients. Increases in the particle size, however, were observed after rehydration of liposomes lyophilized without excipient. On the other hand, liposomes lyophilized with excipients exhibited similar particle sizes before and after freeze-drying, indicating that all the excipients studied stabilized cationic liposomes against aggregation during drying.

Figure 2 shows the storage stability of cationic liposomes lyophilized with the excipients. Increases in particle size were observed during storage at 40 °C except for the trehalose formulation prepared by slow freezing. The liposome formulations containing sucrose, the T_g of which (32 °C) was lower than the storage temperature, were least stable. The formulations containing trehalose, the T_g of which (49 °C) was higher than the storage temperature, were more stable than the sucrose formulations. Addition of dextran to sucrose resulted in a higher T_g (43 °C for 2 : 1 sucrose–dextran mixture and 60 °C for 1 : 1 mixture) and increased the stability of the liposome formulations. These results indicate that the stability of cationic liposome formulations is closely correlated with the mobility of the formulation matrix as indicated by T_g. The formulation containing trehalose prepared by quick freezing exhibited increases in the particle size, but no significant increase was observed for the trehalose formulation prepared by slow freezing, indicating that the storage stability of lyophilized cationic liposomes is affected by the freezing rate.

Figure 3 shows a photograph of lyophilized cationic liposomes containing sucrose or trehalose stored at 25 °C and 23% RH for 1 year. Shrinkage of the freeze-dried cake was observed for sucrose formulations. The extent of shrinkage was larger for the sample prepared by quick freezing. No significant shrinkage of freeze-dried cakes was observed for trehalose formulations and sucrose–dextran formulations (data not shown), which had T_g values higher than those of sucrose formulations. Figure 4 shows the particle size of liposomes after storage at 25 °C and 23% RH for 1 year. The trehalose and sucrose–dextran formulations were stable, but an increase in the particle size was observed for sucrose formulations during storage at 25 °C (approximately 8 °C lower than the T_g of the sucrose formulation). These results indicate that the sucrose formulations have a sufficient degree of matrix mobility to cause liposome aggregation even at 25 °C, a temperature lower than the T_g of the formulation.

Molecular Mobility and Matrix Mobility of Cationic

Table 1. T_g of Lyophilized Cationic Liposome Formulations[a]

Excipient	T_g (°C)[b]	
	Slow freezing	Quick freezing
Sucrose	32.3	31.9
Trehalose	48.4	49.0
Suc–Dex (2 : 1)	43.5	43.7
Suc–Dex (1 : 1)	59.7	59.9

a) Water content was adjusted by storage at 25 °C and 23% RH for 1 d. *b*) T_g values reported were average of two determinations.

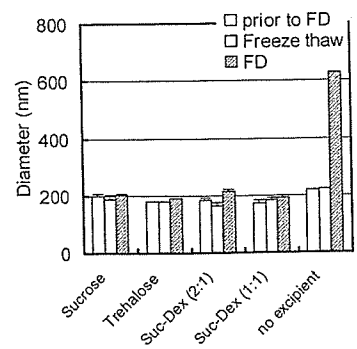

Fig. 1. Effect of Freeze-Thaw and Freeze-Drying on the Particle Size of Cationic Liposomes

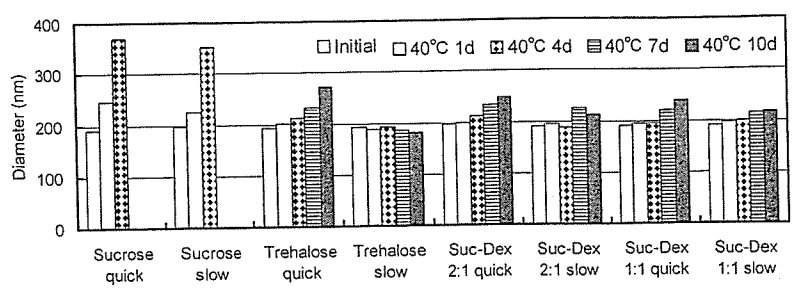

Fig. 2. Effect of Storage at 40 °C on the Particle Size of Cationic Liposomes

Liposome Formulations The storage stability of lyophilized cationic liposomes was affected by freezing rate, such that formulations prepared by quick cooling were less stable than those prepared by slow cooling, as shown in Figs. 2—4. To gain an insight into the mechanism of the effect of freezing rate on the stability of cationic liposome formulations, the mobility of the formulation matrices was examined by ^{1}H-NMR relaxation and shear relaxation measurements. Table 2 shows the T_1 and $T_{1\rho}$ of cationic liposome formulations. T_1 and $T_{1\rho}$ are measures of molecular mobility on time scales of the order of MHz and mid kHz, respectively.[9] T_1 and $T_{1\rho}$ of the formulations did not change with freezing rate within experimental error, indicating that freezing rate has little effect on the molecular mobility reflected in T_1 and $T_{1\rho}$.

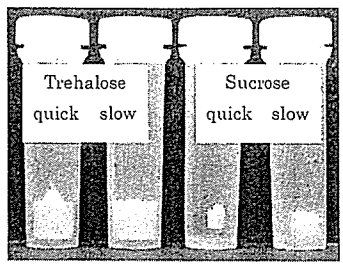

Fig. 3. Appearance of Freeze-Dried Cakes of Cationic Liposomes Containing Sucrose or Trehalose after Storage at 25 °C and 23% RH for 1 Year

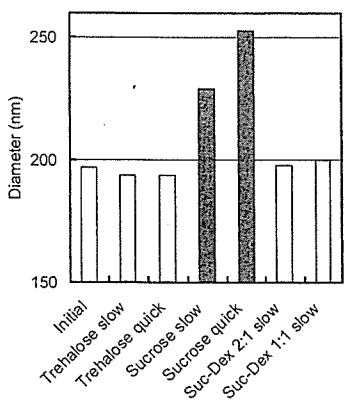

Fig. 4. Effect of Storage at 25 °C and 23% RH for 1 Year on Particle Size of Cationic Liposomes

Table 2. ^{1}H-NMR Relaxation Time of Cationic Liposome Formulations

Excipient		T_1 (s)	$T_{1\rho}$ (ms)
Sucrose	Slow	0.29	4.0
	Quick	0.28	4.0
Trehalose	Slow	0.28	4.4
	Quick	0.30	4.6

The mobility of formulation matrices on longer time scales than those reflected in NMR spin–lattice relaxation times was determined by measuring the frequency dependence of the shear modulus of lyophilized cationic liposomes (the visco-elastic property of the formulations). The frequency-dependent shear modulus ($G^*(\omega)$) of amorphous indomethacin has been shown to characterize the time scales of molecular motion of indomethacin in the amorphous state.[10] The storage modulus (G', a real part of $G^*(\omega)$) of visco-elastic materials increases with increasing frequency of shear stress, and the loss modulus (G'', an imaginary part of $G^*(\omega)$) exhibits a maximum. Visco-elastic materials behave as a viscous fluid and a rigid solid against low and high frequency stress, respectively. The shear relaxation time, the reciprocal of maximum frequency (in radian/s) of G'', can be used as a measure of mobility. Figure 5 shows the typical frequency dependence of the shear modulus of the cationic liposome formulation containing sucrose measured at 74 °C in the dry state. Figure 6 shows the temperature dependence of shear relaxation time for the cationic liposome formulations containing sucrose and trehalose measured under dry conditions. The relaxation time of the formulation prepared by slow freezing was longer than that of the formulation prepared by quick freezing. The effect of freezing rate on the shear relaxation time was also observed in the presence of moisture. Figure 7 shows the frequency dependence of G'' for the cationic liposome formulation containing sucrose stored at 25 °C and 23% RH for 1 d. The formulation prepared by

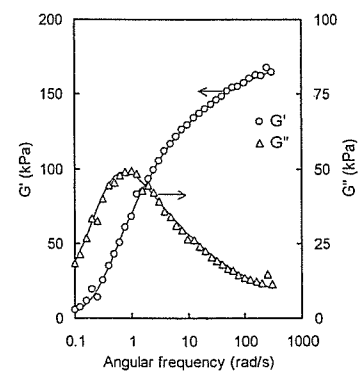

Fig. 5. Frequency Dependence of the Shear Modulus of a Cationic Liposome Formulation Containing Sucrose Measured at 74 °C in the Dry State

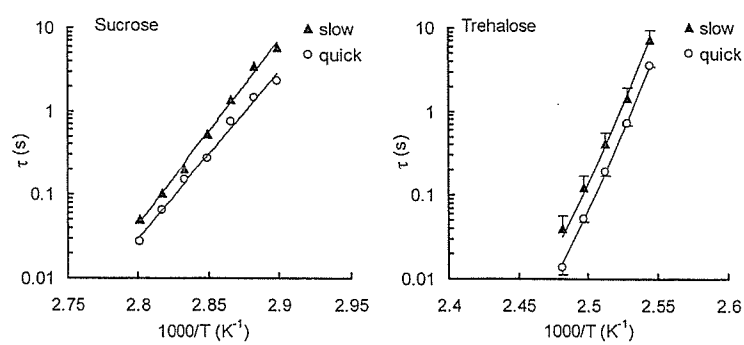

Fig. 6. Shear Relaxation Time of Cationic Liposome Formulations Measured under Dry Conditions

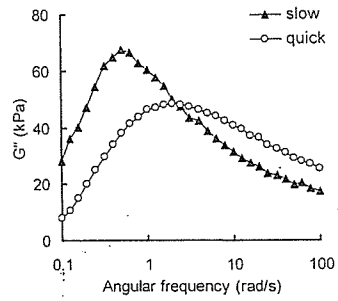

Fig. 7. Frequency Dependence of the Loss Modulus (G'') of a Cationic Liposome Formulation Containing Sucrose at 30 °C

The water content was adjusted by storage at 25 °C and 23% RH for 1 d.

quick freezing exhibited a maximum at 2 radian/s, whereas the formulation prepared by slow freezing exhibited a maximum at 0.4 radian/s. These results indicate that formulation matrices prepared by slow freezing have a lower mobility than those prepared by quick freezing. Temperature dependence of G'' supports this speculation. G'' at a frequency of 0.1 radian/s showed a maximum at 21 °C for the sucrose formulation prepared by quick freezing, whereas 26 °C for the sucrose formulation prepared by slow freezing. The maximum temperature corresponds to the temperature at which relaxation time of 10 s (inverse of 0.1 radian/s) is observed. Therefore, the relaxation time at 25 °C is considered to be longer than 10 s for the sucrose formulation prepared by slow freezing. In contrast, shorter relaxation time than 10 s is expected for the sucrose formulation prepared by quick freezing. This difference in matrix mobility resulting from different freezing rates may cause a difference in storage stability. The difference in matrix mobility of cationic liposome formulations prepared by different freezing rates could be detected by shear relaxation time, but not by T_g and ^{1}H-NMR relaxation measurements (Tables 1, 2). This finding suggests that the aggregation rate of lyophilized liposomes may correlate more closely with matrix mobility as measured by the shear relaxation time than with molecular mobility as measured by the spin-lattice relaxation time.

Figure 8 shows the time course of water vapor sorption for the cationic liposome formulations containing sucrose and trehalose stored at 25 °C and 10% RH. The water content at equilibrium was not affected by freezing rate. The weight of the formulations prepared by quick freezing, however, reached a plateau within 40 min, whereas it took more than 300 min to reach equilibrium for formulations prepared by slow freezing. The difference in water sorption rate indicates that the ratio of surface area to volume for the formulations prepared by quick freezing is larger than that for the formulations prepared by slow freezing. Similar differences in the surface area of freeze-dried cakes have been reported for lyophilized tissue-type plasminogen activator formulations.[8] Such dependence of the surface area on freezing rate may cause the different mobility of the formulation matrices, as indicated by the different shear relaxation times. Formulations with lager surface area may be more susceptive to changes in the T_g upon local temperature fluctuations and/or local humidity fluctuations. Differences in the susceptibility may affect the shrinkages of freeze-dried cakes and the stability of liposomes during storage.

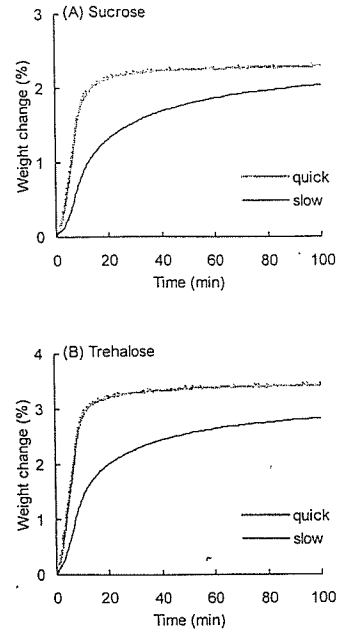

Fig. 8. Time Courses of Water Vapor Sorption of Cationic Liposome Formulations Stored at 25 °C and 10% RH

In conclusion, the storage instability of lyophilized cationic liposomes, as indicated by change in particle size, was affected by the T_g of the formulations. Formulations containing high-T_g excipients exhibited better storage stability. The storage stability of lyophilized cationic liposomes was also affected by freezing rate. Longer shear relaxation times were observed for formulations prepared by slow freezing compared with those prepared by quick freezing, indicating that formulations prepared by slow freezing have a lower matrix mobility. The lower matrix mobility of the formulations prepared by slow freezing may result in better storage stability. T_g or ^{1}H-NMR relaxation measurements could not detect these differences in matrix mobility. Shear relaxation measurements appear to be useful for evaluating the storage stability of cationic liposome formulations.

Acknowledgements A part of this work was supported by a Grant-in-aid for Research on Health Sciences Focusing on Drug Innovation from The Japan Health Sciences Foundation.

References

1) Anchordoquy T. J., Koe G. S., *J. Pharm. Sci.*, **89**, 289—296 (2000).
2) Lai E., van Zanten J. H., *J. Pharm. Sci.*, **91**, 1225—1232 (2002).
3) Li B., Li S., Tan Y., Stolz D. B., Watkins S. C., Block L. H., Huang L., *J. Pharm. Sci.*, **89**, 355—364 (2000).
4) Anchordoquy T. J., Carpenter J. F., Kroll D. J., *Arch. Biochem. Biophys.*, **348**, 199—206 (1997).
5) Molina M. C., Allison S. D., Anchordoquy T. J., *J. Pharm. Sci.*, **90**, 1455—1455 (2001).
6) Crowe J. H., Leslie S. B., Crowe L. M., *Cryobiology*, **32**, 355—366 (1994).
7) van Winden E. C., Zhang W., Crommelin D. J., *Pharm. Res.*, **14**, 1151—1160 (1997).
8) Hsu C. C., Nguyen H. M., Yeung D. A., Brooks D. A., Koe G. S., Bewley T. A., Pearman R., *Pharm. Res.*, **12**, 69—77 (1995).
9) Horii F., "Solid State NMR of Polymers," Chap. 3, ed. by Ando I., Elsevier, Amsterdam, 1998, pp. 51—81.
10) Andronis V., Zografi G., *Pharm. Res.*, **14**, 410—414 (1997).

Glass Transition-Related Changes in Molecular Mobility below Glass Transition Temperature of Freeze-Dried Formulations, as Measured by Dielectric Spectroscopy and Solid State Nuclear Magnetic Resonance

SUMIE YOSHIOKA, YUKIO ASO

National Institute of Health Sciences, 1-18-1 Kamiyoga, Setagaya-ku, Tokyo 158-8501, Japan

Received 27 April 2004; revised 7 September 2004; accepted 14 September 2004

Published online 29 November 2004 in Wiley InterScience (www.interscience.wiley.com). DOI 10.1002/jps.20244

ABSTRACT: The purpose of this study was to explore why changes in the molecular mobility associated with glass transition, the timescale of which is on the order of 100 s, can be detected by measuring the nuclear magnetic resonance relaxation times that reflect molecular motions on the order of 10 kHz and 1 MHz. The molecular motions in freeze-dried dextran 40k, dextran 1k, isomaltotriose (IMT), and α-glucose comprising a common unit but with different glass transition temperatures, were investigated by dielectric spectroscopy (DES) in the frequency range of 0.01 Hz to 100 kHz and in the temperature range of −20° to 200°C, in order to compare with the molecular motions reflected in nuclear magnetic resonance relaxation times. The α-relaxation process for freeze-dried α-glucose was visualized by DES, whereas those for freeze-dried dextran 40k, dextran 1k, and IMT were too slow to be visualized by DES. The latter freeze-dried cakes exhibited quasi-dc polarization because of proton-hopping–like motion rather than α-relaxation process. The correlation time (τ_c) for the backbone carbon of dextran 40k and IMT, calculated from the measured value of spin-lattice relaxation time in the rotating frame, was found to be close to the relaxation time of proton-hopping–like motion determined by DES (τ_{DES}) at temperatures around glass transition temperature. The timescales of molecular motions reflected in the τ_c and τ_{DES} were significantly smaller than that of motions leading to molecular rearrangement (molecular rearrangement motions), which correspond to α-relaxation. However, the shapes of temperature dependence for the τ_c and τ_{DES} were similar to that of the calorimetrically determined relaxation time of molecular rearrangement motions. Results suggest that the molecular motions reflected in the τ_c and τ_{DES} are linked to molecular rearrangement motions, such that enhancement of molecular rearrangement motions enhances the molecular motions reflected in the τ_c and τ_{DES}. Thus, the τ_{DES} and τ_c can reflect changes in molecular mobility leading to unwanted changes in amorphous formulations, and are thought to be a useful measure for evaluating the stability of formulations. J Pharm Sci 94:275–287, 2005

Keywords: dielectric spectroscopy; solid state NMR; freeze-drying; relaxation time

INTRODUCTION

Amorphous pharmaceuticals, as opposed to crystals, reveal various modes of rotational and diffusive motions leading to molecular rearrangement that may bring about unwanted changes in the system. These motions leading to molecular rearrangement (hereafter referred to as molecular rearrangement motions) exhibit an average relaxation time on the order of 100 s at the calorimetric glass transition temperature (T_g). Furthermore, the average relaxation time

Correspondence to: Sumie Yoshioka (Telephone: 81-3-3700-8547; Fax: 81-3-3707-6950; E-mail: yoshioka@nihs.go.jp)

Journal of Pharmaceutical Sciences, Vol. 94, 275–287 (2005)

changes with changing temperature according to the Adam-Gibbs-Vogel (AGV) and Vogel-Tammann-Fulcher (VTF) equations below and above T_g, respectively.[1]

Investigations of the molecular mobility of freeze-dried formulations containing polymer excipients have demonstrated that glass transition occurs partially even at temperatures below T_g, enhancing molecular rearrangement motions and leading to decreases in the physical and chemical stability.[2–6] Changes in the temperature dependence of molecular rearrangement motions associated with the glass transition have been detected by measuring nuclear magnetic resonance (NMR) relaxation times such as laboratory and rotating frame spin-lattice relaxation times (T_1 and $T_{1\rho}$) and spin–spin relaxation time (T_2) of ^1H and ^{13}C.[7–12] However, there is no clear explanation for the question why changes in the temperature dependence of molecular rearrangement motions with a relaxation time longer than 100 s at sub-T_g can be detected by measuring NMR relaxation times such as T_1, $T_{1\rho}$, and T_2 of ^1H and ^{13}C that reflect molecular motions on the order of 1 MHz, 10 kHz, and >10 kHz, respectively. Thus, the aim of this investigation was to elucidate the relationship between molecular rearrangement motions and molecular motions reflected in NMR relaxation times in freeze-dried formulations containing polymer excipients. In an effort for this purpose, molecular motions reflected in NMR relaxation times were first compared with molecular motions reflected in dielectric spectra, which is capable of observing molecular motions ranging from 0.01 Hz to 100 kHz.

Dielectric relaxation spectroscopy (DRS) is a useful method of determining molecular mobility, as is NMR relaxation measurement. NMR measures the fluctuation of a certain atom, whereas DRS measures the reorientation of a molecular dipole. NMR allows determination of the molecular motion of a specific site in the molecule, whereas DRS reflects the mobility of molecular dipoles that are usually difficult to specify in the case of polymers. The correlation time, which represents the timescale of molecular motion, cannot be determined directly from the NMR relaxation time, because NMR relaxation time depends on the relaxation mechanism. Therefore, it is necessary to understand the relaxation mechanism in order to calculate the correlation time from the observed relaxation time. However, DRS is able to directly detect the timescale of molecular motions ranging from 10^{-11} to 10^3 s.

DRS has been used to determine the molecular mobility of various amorphous pharmaceuticals and excipients.[13–16] The mobility of water coexisting with excipients has also been investigated using DRS.[17–22] Montes and Cavaille[16] used DRS to observe the γ- and β-relaxation of dextran film, which were assigned to the noncooperative motion of local segments and the cooperative motion of main chain segments, respectively, based on the observed activation energy. Noel et al.[14] observed the α-relaxation of amorphous glucose corresponding to molecular rearrangement motions by DRS.

In this investigation, the molecular motions in freeze-dried dextran 40k, dextran 1k, isomaltotriose (IMT), and α-glucose comprising a common unit but with different T_g's, were first investigated by dielectric spectroscopy (DES). Then, the temperature dependence of the relaxation time determined by DES (τ_{DES}) was compared with that of the correlation time determined by NMR relaxation measurements (τ_c), in order to discuss the relationship between the molecular motions detected by DES and NMR. The τ_c for the backbone carbon of freeze-dried IMT was calculated from the $T_{1\rho}$ value measured in this study, and that of freeze-dried dextran 40k was calculated from the $T_{1\rho}$ value reported previously.[11] Furthermore, the τ_c and τ_{DES} were compared with the timescale of molecular rearrangement motions measured calorimetrically, in order to discuss the correlation of molecular rearrangement motions and molecular motions reflected in the τ_c and τ_{DES}.

EXPERIMENTAL

Freeze-Drying

Freeze-dried samples for DES measurement were prepared as follows: each of dextran 40k (D-4133; Sigma Chemical Co.), dextran 1k (00268; Fluka Production GmbH), IMT (I-0381; Sigma Chemical Co.), and α-D-glucose (anhydrous 158968; Aldrich) was dissolved in distilled water (5% w/w). Conversion of α-D-glucose to β-D-glucose during the dissolution was prevented by cooling the solution with ice. Seven hundred microliters of the solutions was frozen in a polypropylene sample tube (17-mm diameter) by immersion in liquid nitrogen for 10 min, and then dried at a vacuum level below 5 Pa for 23.5 h in a lyophilizer (Freezevac C-1; Tozai Tsusho Co., Tokyo). The shelf temperature was between −35° and −30°C for the first 1 h, 20°C for the subsequent 19 h, and 30°C for the last 3.5 h.

Table 1. T_g of Freeze-Dried Cakes Determined using Differential Scanning Calorimetry

	Dry	23% RH	43% RH	60% RH	75% RH
Dextran 40k	230°C		80	58	35
Dextran 1k	167				
IMT	122	53	33	7	
α-Glucose	35				

To prepare freeze-dried samples for $T_{1\rho}$ measurement, 400 μL of IMT solution (2.5% w/w) was frozen in a polypropylene sample tube (10-mm diameter).

Freeze-dried samples with various water contents were obtained by storing the freeze-dried sample at 15°C for 24 h in a desiccator with a saturated solution of potassium acetate [23% relative humidity (RH)], K_2CO_3 $2H_2O$ (43% RH), NaBr $2H_2O$ (60% RH), or NaCl (75% RH). The T_g of samples was determined by differential scanning calorimetry at a scan rate of 20°C/min (2920; TA Instruments, New Castle, DE), and the results are shown in Table 1.

DES

Dielectric measurements were performed with a dielectric analyzer (model 2970; TA Instruments) operating in the frequency range of 0.01 Hz to 100 kHz and in the temperature range of −20° to 200°C. Gold parallel plate electrodes (ceramic parallel plate, 25 mm) were used. Permittivity was measured with and without a thin Teflon sheet (0.2-mm thickness) inserted between the sample and the upper electrode. The Teflon sheet was used to inhibit charge transfer between the electrode and the sample, as reported for measurement of the Maxwell-Wagner process in a heterogeneous dielectric mixture.[18] Teflon was chosen because of the low permittivity and the lack of dielectric dispersion in the temperature and frequency range examined. The observed values of real permittivity (ε′) and imaginary permittivity (ε″) were relative rather than absolute, because the electrode area, which was larger than the sample area, was used for the calculation of permittivity. Therefore, the ratio of ε″ to ε′ (tan δ) was calculated as a parameter independent of the surface area of the sample.

For measurement in the dry state, lyophilized cakes were placed on the lower electrode, and the chamber enclosing the sample was purged with nitrogen gas for 24 h at a constant temperature (120°C for dextran 40k, 100°C for dextran 1k and IMT, and 25°C for α-glucose). A small container of P_2O_5 was introduced into the chamber for measurement of α-glucose samples. After removing moisture, samples were compressed with a force of 500 N, and permittivity was measured at a constant temperature as a function of frequency. Permittivity was also measured at a constant frequency of 1 Hz and 1 kHz as a function of temperature. Heating rate was 5°C/min for dextran 40k, dextran 1k, and IMT, and 20°C/min for α-glucose (rapid measurement to prevent glucose crystallization during the measurement).

Permittivity of the samples containing moisture was measured at 25°C as a function of frequency, immediately after placing the cake (pre-equilibrated at 23%, 43%, 60%, or 75% RH) on the lower electrode (500 N).

Determination of $T_{1\rho}$ by ^{13}C Solid State NMR

The $T_{1\rho}$ of methine carbon in the IMT backbone (Fig. 1) was determined for the peak at 70 ppm (Fig. 2) at temperatures ranging from 5° to 65°C

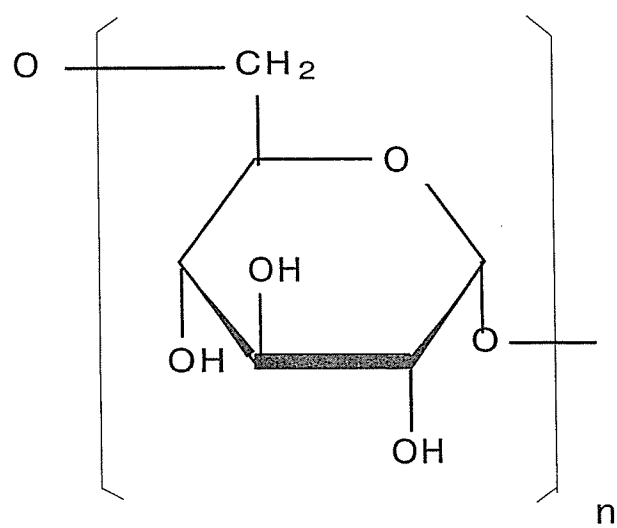

Figure 1. Repeated unit of α-glucose series.

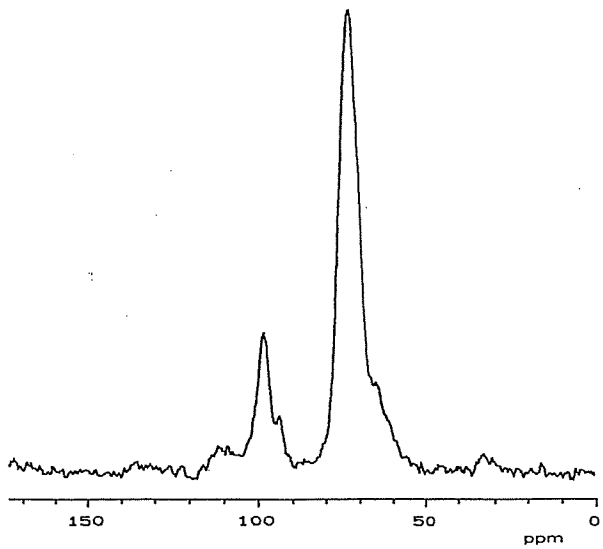

Figure 2. NMR spectrum of lyophilized IMT equilibrated at 43% RH, measured at 25°C and 1 ms of spin-locking duration.

with freeze-dried IMT equilibrated at 43% and 60% RH, using a UNITY plus spectrometer operating at a proton resonance frequency of 400 MHz (Varian Inc., Palo Alto, CA), as previously described.[11] Spin-locking field was equivalent to 57 kHz. The rotor size was 7 mm and spinning speed was 4 kHz. Signal decay was describable with a mono-exponential equation.

RESULTS AND DISCUSSION

Molecular Motions Observed by DES

Figure 3 shows the temperature dependence of the tan δ observed for freeze-dried dextran 40k. The tan δ measured with a Teflon sheet inserted is also shown in Figure 3. The tan δ exhibited a peak around 130°C when measured at 1 Hz with a Teflon sheet inserted (Fig. 3A), but increases in tan δ were only observed in the absence of the Teflon sheet (Fig. 3B). The peak for β-relaxation of dextran 40k is expected to appear below 27°C at 1 kHz, because β-process was observed at 27°C for a film of a larger molecular weight dextran.[16] Therefore, the changes in tan δ observed at 1 kHz (Fig. 3A), the peak of which is expected to appear above 200°C, were attributed to another process that is slower than the β-process.

Figure 4 shows the temperature dependence of tan δ observed at 1 kHz for freeze-dried α-glucose, IMT, and dextran 1k, together with that observed for freeze-dried dextran 40k. Freeze-dried IMT

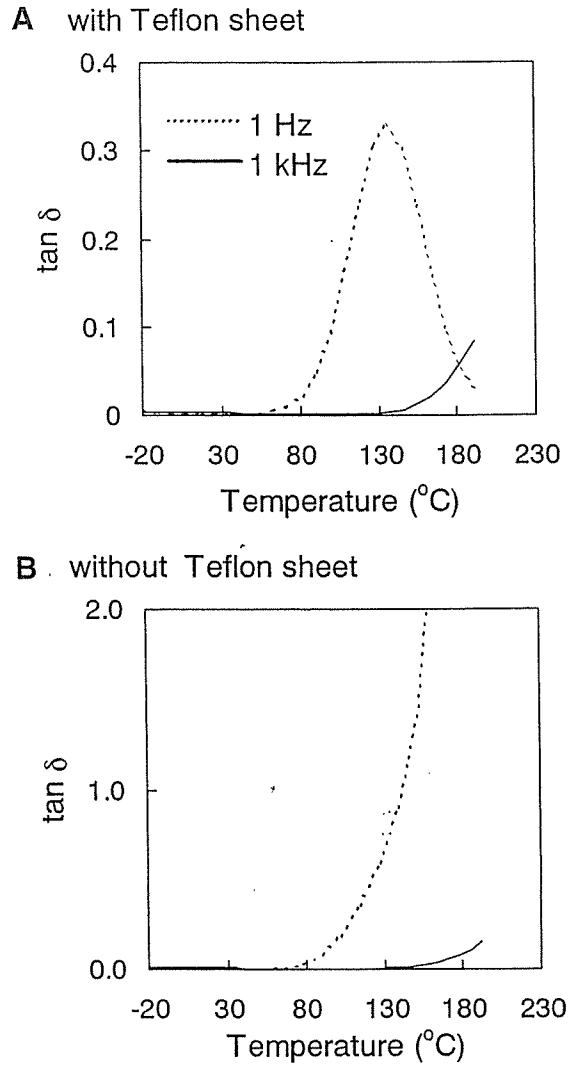

Figure 3. Temperature dependence of tan δ measured for freeze-dried dextran 40k with (A) and without (B) a Teflon sheet at 1 Hz (dashed line) and 1 kHz (solid line).

and dextran 1k exhibited a peak with a Teflon sheet inserted, around 140° and 170°C, respectively (Fig. 4A). This peak was not observed in the absence of the Teflon sheet (Fig. 4B). The increases in tan δ with increasing temperature observed without the Teflon sheet may be attributable to the quasi-dc polarization (referring to low-frequency dispersion accompanied by abnormal increases in permittivity), as reported for hydrated granular or porous solids.[23] This was thought to be because both ε′ and ε″ measured as a function of frequency revealed a substantial increase in the low-frequency region (data not shown). Insertion of a Teflon sheet to inhibit charge transfer into the

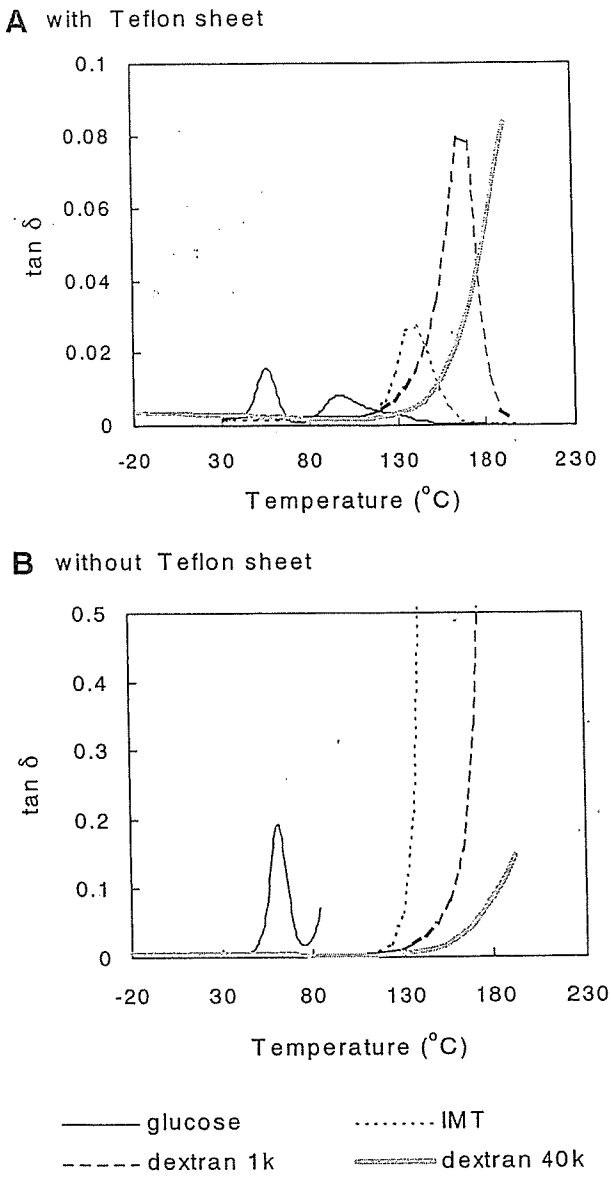

Figure 4. Temperature dependence of tan δ measured for freeze-dried α-glucose, IMT, dextran 1k, and dextran 40k with (A) and without (B) a Teflon sheet at 1 kHz.

electrode enabled the observation of quasi-dc polarization as a peak, in a similar manner as the Maxwell-Wagner process reported for a heterogeneous dielectric mixture.[18]

The mechanism of the observed quasi-dc polarization remains unclear. Quasi-dc polarization has been ascribed to diffusion of ions over the surface of the solid, as reported for hydrated mannitol,[17] or to the proton hopping reported for hydrated proteins.[18,24,25] However, the quasi-dc process observed for freeze-dried α-glucose series cannot be attributed to the hopping of protons in the ionizable carboxylic group as observed in a hydrated protein. A possible explanation for the observed quasi-dc polarization is that a proton-hopping–like process occurs in the hydrogen-bonded network constructed between hydroxy groups in the glucose unit in the form of clusters. However, there still seems to be a question whether such proton-hopping–like process is possible in the nearly dry state.

The frequency at which ε″ shows a maximum value depends on the thickness and permittivity of the sheet used, but can be regarded as a measure for comparing the mean relaxation time of the observed Maxwell-Wagner–like process, namely, proton-hopping–like process. In the freeze-dried IMT, dextran 1k, and dextran 40k, the ε″ value normalized to that observed at the peak (ε''_p) exhibited a similar shape of dielectric spectrum, as shown in Figure 5. The shape of dielectric spectrum did not vary significantly with changing the temperature both below and above the T_g. The dielectric spectra obtained for the freeze-dried IMT showed relatively large scattering.

Freeze-dried α-glucose exhibited two peaks when a Teflon sheet was inserted (Fig. 4A). The peak for tan δ around 100°C was not observed in the absence of the Teflon sheet, in a similar manner as the peaks observed for IMT, dextran 1k, and dextran 40k (Fig. 4B). In contrast, the tan δ peak around 50°C was not affected by the presence of a Teflon sheet. The peak of ε″ corresponding to this tan δ peak was observed only at temperatures above T_g, when measured in the range from 0.01 Hz to 100 kHz, as shown in Figure 6. Furthermore, the distribution of the ε″ peak was larger than that of proton-hopping–like process observed for IMT, dextran 1k, and dextran 40k. These results suggest that the peak observed for tan δ is attributed to α-relaxation—molecular rearrangement motions that are related to the instability of freeze-dried formulations. Noel et al.[14] observed the α-relaxation of α-glucose at 1 kHz and at 70°C, which was higher than the temperature reported herein. This difference in temperature may be attributable to the difference in the water content of the samples.

The other peak observed around 100°C (Fig. 4A) seems to be attributed to a charge transfer process, similar to the proton-hopping–like process observed for IMT, dextran 1k, and dextran 40k, because it was not observed without the Teflon sheet (observed ε′ values were negative at temperatures above 85°C) (Fig. 3B). However, the